7

Tropical cyclones and climate change: revisiting recent studies at GFDL

THOMAS R. KNUTSON AND ROBERT E. TULEYA

Condensed summary

In this chapter, we revisit two recent studies performed at the Geophysical Fluid Dynamics Laboratory (GFDL), with a focus on issues relevant to tropical cyclones and climate change. The first study was a model-based assessment of twentieth-century regional surface temperature trends. The tropical Atlantic Main Development Region (MDR) for hurricane activity was found to have warmed by several tenths of a degree Celsius over the twentieth century. Coupled model historical simulations using current best estimates of radiative forcing suggest that the century-scale warming trend in the MDR may contain a significant contribution from anthropogenic forcing, including increases in atmospheric greenhouse gas concentrations. The results further suggest that the low-frequency variability in the MDR, apart from the trend, may contain substantial contributions from both radiative forcing (natural and anthropogenic) and internally generated climate variability. The second study used the GFDL hurricane model, in an idealized setting, to simulate the impact of a pronounced CO_2-induced warming on hurricane intensities and precipitation. A 1.75 °C warming increases the intensities of hurricanes in the model by 5.8% in terms of surface wind speeds, 14% in terms of central pressure fall, or about one half category on the Saffir–Simpson Hurricane Scale. A revised storm-core accumulated (six-hour) rainfall measure shows a 21.6% increase under high-CO_2 conditions. Our simulated storm intensities are substantially less sensitive to sea surface temperature (SST) changes than recently reported historical observational trends are – a difference we are not able to completely reconcile at this time.

7.1 Introduction

In a recent study (Knutson and Tuleya, 2004; hereafter referred to as KT04), we reported results from an extensive set of idealized hurricane model

Climate Extremes and Society, ed. H. F. Diaz and R. J. Murnane. Published by Cambridge University Press.

simulations that explored the impact of a substantial CO_2-induced climate warming on hurricane intensities and precipitation. We found increased hurricane intensities under warmer climate conditions, with an average maximum surface winds sensitivity of 5.8%, for an average sea surface temperature (SST) increase of 1.75 °C. Since that paper was published, several provocative observational studies have appeared (e.g., Emanuel, 2005a; Webster *et al.*, 2005; Mann and Emanuel, 2006) that presented some evidence for increasing trends in intensity-related tropical cyclone measures in historical observations.

In this study, we review our earlier work (Section 7.3) and discuss the prospects for reconciling our earlier results with the recently reported observed trends of hurricane intensity measures (Section 7.4). We also present some further analysis of precipitation from the KT04 experiments (Section 7.3), through which we find that a recently identified analysis problem with our original inner-core precipitation measure – when properly addressed – has little impact on the percent changes in inner-core rainfall rates under high-CO_2 conditions as reported in KT04 (although it does affect the absolute values of the precipitation rates).

In a separate recent study, Knutson *et al.* (2006; hereafter referred to as K06) used a new, coupled ocean–atmosphere climate model to assess potential causes of twentieth-century surface temperature trends in a number of regions. With regard to tropical cyclone behavior, a potentially important result emerging from this study was the identification of a century-scale surface warming trend in the tropical Atlantic Main Development Region (MDR). The model assessment results suggest that this warming may contain a significant contribution from anthropogenic forcing, including increasing greenhouse gas concentrations. In this chapter, the K06 analysis related to the MDR warming trends is reviewed and expanded upon (Section 7.2).

7.2 Tropical Atlantic (Main Development Region) temperature trends

The region of the tropical North Atlantic and Caribbean extending from 10° N to 20° N is often referred to as the Main Development Region (MDR) for Atlantic hurricane activity, owing to the large portion of major hurricanes that can be traced to disturbances originating there (e.g., Goldenberg *et al.*, 2001; Bell and Chelliah, 2006). Here we explore possible causes for a warming of this region during the twentieth century. Shown in Figure 7.1 are 10-year running mean surface temperature indices for the MDR and for the globe obtained from the HadCRUT3 combined SST/land surface air temperature dataset (www.cru.uea.ac.uk/cru/data/temperature/; Parker *et al.*, 1995; Jones and Moberg, 2003; Rayner *et al.*, 2003; Brohan *et al.*, 2006).

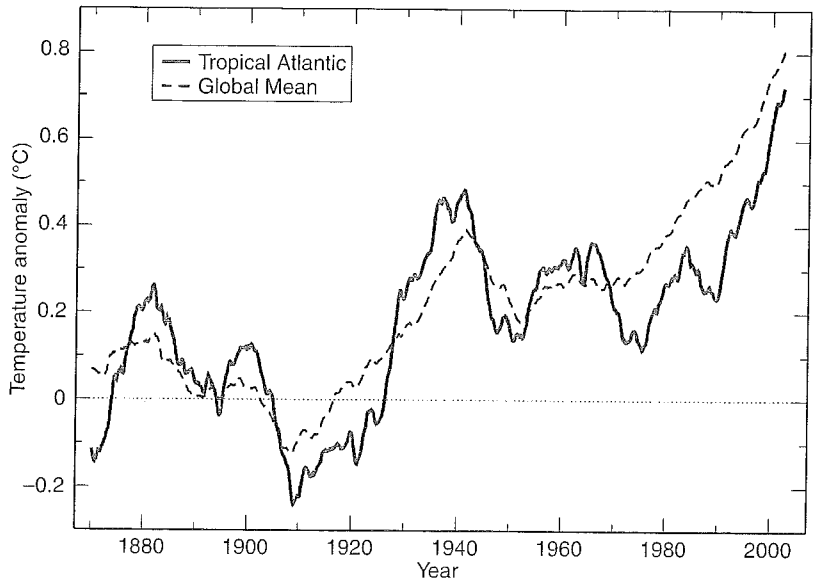

Figure 7.1. Ten-year running mean surface temperature anomalies for the Tropical Atlantic Main Development Region and global average. The MDR is defined here as the region 10° N–20° N, 80° W–20° W. The dataset used is the combined land–ocean HadCRUT3. Anomalies (in degrees Celsius) have been adjusted to have zero mean for the period 1881–1920.

Low-frequency surface temperature variability in the MDR is dominated by sea surface temperature variability in this predominantly oceanic region. The surface temperature data indicate that the MDR warmed by several tenths of a degree Celsius over the twentieth century (Figure 7.1). This warming has been noted previously (e.g., Emanuel, 2005a; Trenberth, 2005; K06; Santer *et al.*, 2006). The MDR warming roughly tracks the increase in global mean surface temperature, but with larger multidecadal swings in temperature compared with those in the global mean record. Concerning the global mean temperature increase, a large body of research has assessed the possible role of increasing greenhouse gases on global mean temperature (e.g., Meehl *et al.*, 2004; International Ad Hoc Detection and Attribution Group [IADAG], 2005; K06) and concludes that most of the global warming over the past 50 years is likely due to the increase in greenhouse gases. Fewer studies have addressed this question on regional scales such as the MDR. Santer *et al.* (2006) recently examined warming trends in both the Atlantic and Pacific tropical cyclogenesis regions using 22 different climate models and concluded that there is an 84% chance that external forcing led to at least two-thirds of the observed SST increases in these regions.

In another recent model-based assessment (K06) observed twentieth-century surface temperature trends in the MDR and various other regions

were compared with trends obtained by using two new Geophysical Fluid Dynamics Laboratory (GFDL) global climate models. Three different historical climate-forcing scenarios were examined (see below). Current best estimates of a number of historical climate forcings over the period 1860–2000 were specified for these scenarios. The forcings included representations of greenhouse gases, volcanic eruptions, solar variability, land cover changes, and aerosols. These forcings were incorporated more realistically than those used in previous GFDL coupled climate model experiments (e.g., Broccoli *et al.*, 2003). The aerosol forcing included the "direct effect" only and did not include effects of interactions of aerosols with clouds or precipitation processes.

Figure 7.2 shows late summer sea surface temperatures in the MDR as simulated in the K06 historical runs compared with observations from the HadISST (Rayner *et al.*, 2003) and ERSST.v2 (Smith and Reynolds, 2003, 2004) datasets. The top panel (Figure 7.2a) shows the observed MDR series in comparison to an eight-member ensemble of experiments, which used both anthropogenic and natural historical forcings (i.e., all available forcings). Natural forcings (Figure 7.2b) include only volcanic aerosols and long-term variability of solar radiation. Anthropogenic forcings (Figure 7.2c) include only changes in well-mixed greenhouse gases, ozone, aerosols, and land cover. Further details on these forcings are provided in K06. The differences among the ensemble members for each forcing scenario reflect internal climate variability as simulated by the model. Each ensemble member is initialized with different ocean initial conditions taken from a multi-century, 1860-condition control run, and thus begins in a different phase in terms of internally generated modes of the model, such as the model's El Niño, North Atlantic Oscillation (NAO), or internal Atlantic Ocean variability.

In the MDR, the observed long-term warming during the twentieth century is much more realistically simulated in the model runs, which include anthropogenic forcing (i.e., the all-forcing or anthropogenic-only-forcing scenarios) than in the natural-forcing runs. This is particularly true for the late twentieth-century warming. There is some resemblance of the temporal structure of the all-forcing ensemble mean compared to the observations beyond just the century-scale linear trend. However, the observations still exhibit pronounced multidecadal departures from the ensemble mean of the all-forcing runs. The anthropogenic-forcing ensemble mean response (c; $n = 4$) in the MDR appears fairly linear. A more nonlinear response (increasing slope over time) is evident for the global mean results (see K06, Fig. 1e). The anthropogenic- and all-forcing runs include only the direct effect of aerosols, and so the total forcing from aerosol changes (including indirect effects) is

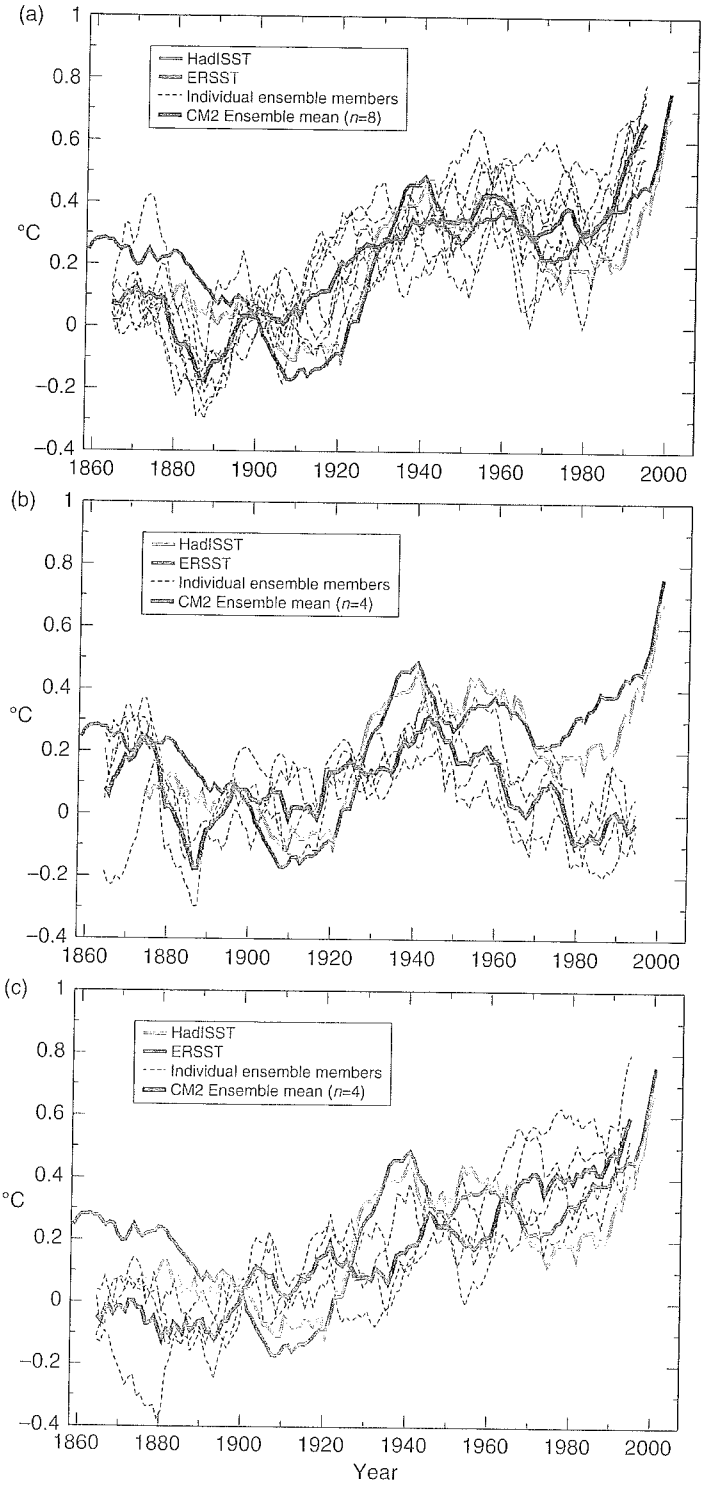
(a)
HadISST
ERSST
Individual ensemble members
CM2 Ensemble mean (n=8)
°C
(b)
HadISST
ERSST
Individual ensemble members
CM2 Ensemble mean (n=4)
°C
(c)
HadISST
ERSST
Individual ensemble members
CM2 Ensemble mean (n=4)
°C
1
0.8
0.6
0.4
0.2
0
−0.2
−0.4
1860
1880
1900
1920
1940
1960
1980
2000
Year

likely underestimated. The natural-forcing ensemble (b; $n = 4$) indicates a significant role for volcanic activity in producing some of the low-frequency structure in the all- and natural-forcing simulations. Similar results to these, although with less internal variability, were obtained for other regions, such as annual-mean global mean temperature, in K06. These results are generally consistent with a multi-model analysis of a region similar to our MDR by Santer *et al.* (2006), who also show reasonable agreement of twentieth-century all-forcing runs with observations, and a notable secondary impact of volcanic eruptions.

Further analysis of the MDR warming was presented in K06, where maps of observed trends over the periods 1901–2000 and 1949–2000 were quantitatively compared to model forcing scenarios and internal variability, using local *t*-tests. In the MDR and vicinity, the 1901–2000 warming trends (based on annual means) were generally significantly larger than the model's internally generated variability, and significantly different from trends in the natural-forcing runs. In contrast, these trends were not significantly different from model trends in forcing runs that included anthropogenic forcing. For the more recent period (1949–2000), the relatively smaller observed trends in the MDR and vicinity were not distinguishable from the model's internal variability, highlighting the fact that a longer (century-scale) record is useful for distinguishing a long-timescale warming trend from other climate variations in the MDR. The relatively cool SSTs in the MDR in the first half of the twentieth century, combined with generally warmer SSTs in the second half of the century, produce a pronounced century-scale warming trend that is larger than expected from internal climate variability or natural forcing alone, according to the model-based assessment. The model-observation statistical comparisons in K06 are limited to periods ending in the year 2000, since the CM2.1 historical model runs performed for K06 ended with that year. The observed low-pass filtered results in Figure 7.2 show a continued strong warming past 2000 (here using data through 2005), which serves to strengthen

Caption for Figure 7.2. Observed sea surface temperature variations in the MDR from HadISST (red) and ERSST (blue) datasets vs. CM2 historical climate simulations using (a) all forcings, (b) natural forcings only, or (c) anthropogenic forcings only. Ten-year running mean anomalies for the August–October season, referenced to 1881–1920 means in degrees Celsius, are shown. Black dashed curves are individual CM2.0 or CM2.1 ensemble members; thick black curves are the CM2.0/CM2.1 ensemble means ($n = 8$ experiments with all forcings; $n = 4$ experiments with natural- or anthropogenic-only forcings). For color version, see plate section.

the conclusions of K06 concerning the unusual nature of this warming compared with internal or natural climate variability.

In total, the results in K06 and in Figures 7.1 and 7.2 here suggest that the century-scale warming trend in the MDR may contain a significant contribution from anthropogenic forcing, including increases in atmospheric greenhouse gas concentrations. Furthermore, the model results suggest that the low-frequency variability in the MDR, apart from the trend, may contain substantial contributions from both radiative forcing (both natural and anthropogenic) and internally generated climate variability. Further work is under way to explore the relative roles of these factors – a topic of recent debate (e.g., Goldenberg *et al.*, 2001; Mann and Emanuel, 2006; Trenberth and Shea, 2006).

The observed and simulated (all-forcing) twentieth-century warming of the MDR is actually part of a much broader-scale warming pattern (e.g., Fig. 7 of K06), spanning both the Northern and Southern Hemispheres. This argues against the notion that the observed global-scale twentieth-century warming is primarily due to fluctuations in the Atlantic thermohaline circulation (THC). For example, Zhang and Delworth (2005) simulated the surface temperature response associated with a pronounced weakening of the Atlantic THC, and showed generally opposite-signed anomalies between the two hemispheres. This contrasts with the general twentieth-century warming trend evident in both hemispheres for both the observations and model simulations.

Another related finding in K06 was the very pronounced observed warming trend in the Indian Ocean – western Pacific warm pool region: an even stronger warming signal than that in the Atlantic MDR. As with the MDR, the model assessment results suggested that anthropogenic forcing has played a significant role in the Indian Ocean – western Pacific warming.

The long-term warming that has occurred in various tropical ocean regions is relevant to our discussion of tropical cyclone intensities in light of the strong correlation between tropical SSTs and several tropical cyclone measures, as has been reported by Emanuel (2005a), Webster *et al.* (2005), Hoyos *et al.* (2006), and Mann and Emanuel (2006) for several tropical ocean basins. The reliability of the tropical cyclone databases used to infer these relationships has been questioned (e.g., Landsea *et al.*, 2006). According to Landsea (2005; 2007), the reliability of basin-wide tropical cyclone statistics for the Atlantic basin decreases as one goes back in time, particularly in the pre-satellite era. Longer records, extending back to 1900, of tropical cyclone intensity measures for US landfalling tropical and subtropical systems have also been examined (e.g., Landsea 2005) but show no apparent trend over the period, in contrast to the MDR SSTs shown in Figures 7.1 and 7.2. However, Emanuel (2005b) noted that US landfalling storm statistics are composed of only a very small fraction of

tropical cyclone observations over the whole basin, and thus any trends present could well be masked by noise effects due to the small sample size.

7.3 Review of KT04 results

7.3.1 Methodology for idealized hurricane simulations

In KT04, we used an idealized simulation approach to investigate the impact of CO_2-induced warming on hurricane precipitation and intensity. The model used was an idealized version of the GFDL Hurricane Prediction System, which has been run operationally for hurricane prediction at the US National Centers for Environmental Prediction (NCEP) for several years. The model has variable resolution, with grid spacing of about 9 km in a $5° \times 5°$ fine-mesh grid that moves with the hurricane through a larger coarse-grid domain. No ocean coupling was used in the experiments. Knutson *et al.* (2001) found that the inclusion of ocean coupling has a minimal impact on the percentage increases in hurricane intensity simulated for warm climate conditions in such experiments. In the idealized experiments, the hurricanes were simulated for 5 days as they traveled over a uniform sea surface (no land) in a large-scale atmospheric environment consisting of a uniform $5\,m\,s^{-1}$ easterly flow. Therefore, no effects of the storms' interactions with land, topography, vertical wind shear,[1] or large weather systems were included in our experimental design. KT04 (its Fig. 15) found that climate model-projected changes in Atlantic basin vertical wind shear in response to increasing CO_2 were quite model-dependent in the nine climate models they examined, although the changes were not very dramatic, even for the most sensitive models. Vecchi and Soden (2007) recently reported that increased vertical wind shear in the Caribbean was a response appearing consistently in most twenty-first-century projections using a newer set of climate models.

To specify the large-scale SSTs, atmospheric temperatures, and atmospheric moisture conditions for our hurricane model experiments, we obtained present-day and high-CO_2 climatologies from nine global climate models, which took part in the international Coupled Model Intercomparison Project (CMIP2+). The high-CO_2 environments were based on the control run climatologies plus 80-year net linear trends from +1% per year compounded CO_2 experiments run for each model (KT04). The present-day conditions were based on 80-year averages from the models' control runs

[1] Vertical wind shear refers to a change in wind speed and/or direction with height. Larger values of vertical wind shear are believed to be detrimental for tropical cyclone development, as they disrupt the vertical organization of the storm.

with constant (present-day) CO_2 levels. A 1% per year compounded increase of CO_2 is a strong, though not extreme, idealized future global radiative forcing scenario (Knutson and Tuleya, 2005). For each climate model, we obtained area-averaged climatologies for the Atlantic, northeastern Pacific, and northwestern Pacific tropical storm basins, in each case time-averaged over the months of July through November.

In addition to sampling high-CO_2 climate states from nine global models, we also tested four different moist physics options in the GFDL hurricane model to assess the potential impact of changes in the treatment of precipitation processes – a crucial process for tropical cyclones – on our simulation results. The four treatments included two mass flux schemes, one convective adjustment scheme, and resolved convection (i.e., using no convective parameterization in the fine-scale inner grid). For each combination of climate model and hurricane model physics, we conducted experiments for two climate states (present-day and high-CO_2), and three basins (Atlantic, northwestern Pacific, and northeastern Pacific). The three basins, nine models, and four moist convection physics treatments yielded $3 \times 9 \times 4 = 108$ configurations to test for each climate state. For each of the 108 configurations, we ran a six-member ensemble of experiments, differing only in terms of small random perturbations to the atmospheric initial conditions for the five-day runs. Thus, in all we ran 1,296 simulations (108 configurations $\times$ 2 climates $\times$ 6 ensemble members). The initial disturbance used was based on a fairly robust initial hurricane condition (maximum wind speeds of approximately 35 m s^{-1}) at a radius of 55 km.

The SST changes for the three tropical cyclone basins obtained from the nine CMIP2+ global models averaged 1.75 °C, with a range of 0.8 °–2.4 °C across the 27 (3 basins $\times$ 9 models) samples. A prominent feature of the tropical climate changes in these global models was an enhancement of the warming in the upper troposphere, relative to the warming at the surface (Figure 7.3). This "tropospheric stabilization" effect has been shown by Shen *et al.* (2000) to reduce the intensity of simulated hurricanes in the GFDL model. On the other hand, warmer SSTs led to more intense storms in their study. A key purpose of our experiments was to use the hurricane model to simulate which of these two effects dominates in a CO_2-induced climate-warming scenario. Our results show that the SST warming effect (increased intensity) exceeds the tropospheric stabilization effect (decreased intensity), yielding a net increase of hurricane intensity in almost all (107 out of 108) ensemble mean combinations examined, as is discussed in detail below.

Further details on all aspects of our models, the CO_2-induced changes in the tropical mean environments from the CMIP2+ models, and other experimental design considerations are contained in KT04.

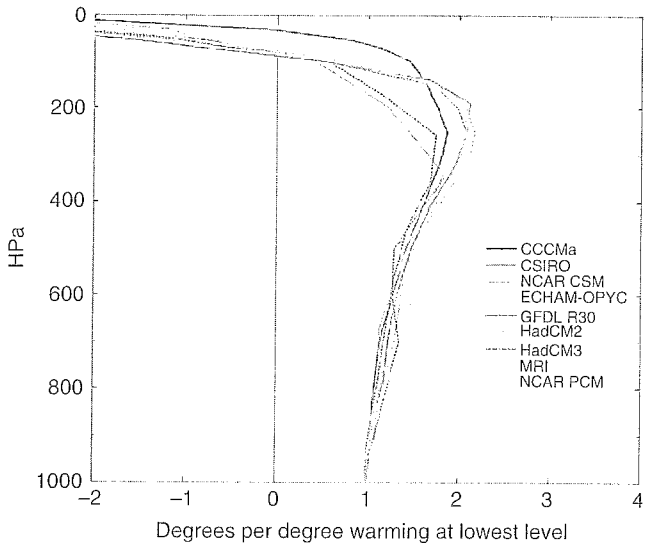

Figure 7.3. Vertical profiles of normalized atmospheric temperature change (high-CO_2 minus control) zonally averaged over 20° N–20° S from a set of transient +1% per year CO_2 increase experiments using nine global climate models. The difference is based on years 61–80 of the high-CO_2 runs minus years 61–80 of the control runs for each model (see legend). The difference at each model level is normalized by dividing by the difference at the lowest available level for that model. For color version, see plate section.

7.3.2 Intensity simulation results

The maximum hurricane intensity (minimum central pressure) results from the 1,296 five-day experiments are summarized in Figure 7.4. The light curve shows the distribution of minimum central pressures (one per simulated storm) obtained for the control (present-day) conditions. The dark curve shows the distribution for the high-CO_2 conditions. The high-CO_2 distribution is shifted systematically to the left, toward lower pressures and higher intensities, compared with the control. The size of the shift is 10.4 millibars (mb) for the mean, and represents about a one half category shift on the Saffir–Simpson Hurricane Scale. Substantially more storms in our idealized experiments reached category 5 for the high-CO_2 conditions than for the control conditions. Although our experiments did not address the question of possible future changes in storm frequency, they did suggest an increasing relative risk in the occurrence of category 5 hurricanes under high-CO_2 conditions. Analysis of subsets of experiments indicated that the increased simulated intensity occurred for nearly all combinations (107 out of 108) of climate model boundary condition, tropical storm basin, and hurricane model moist convection treatment tested. The simulated hurricane intensity increase was

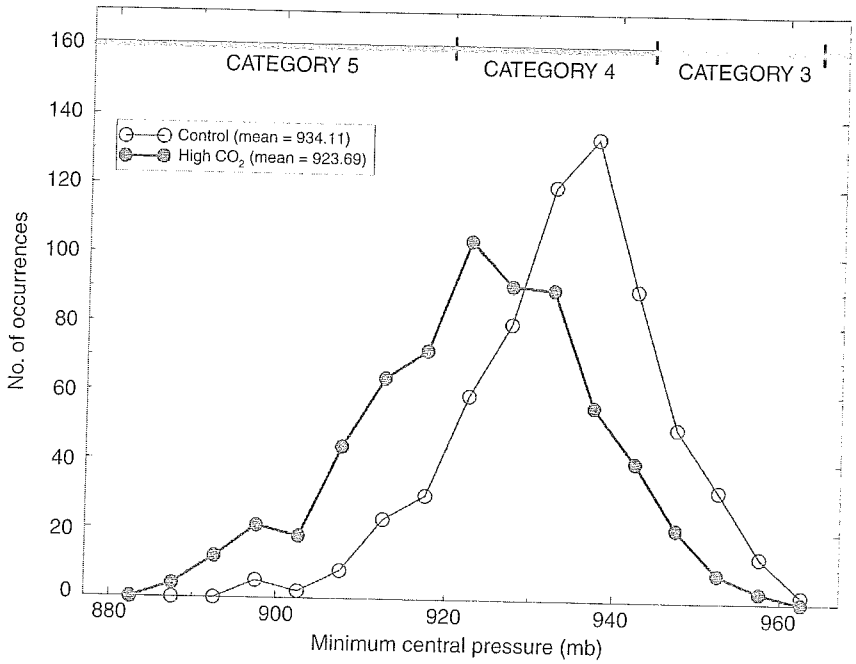

Figure 7.4. Frequency histogram showing hurricane intensity results (millibars) aggregated across all 1,296 experiments of KT04 (9 GCMs, 3 basins, 4 parameterizations, 6-member ensembles). The histograms are formed from the minimum central pressures, averaged over the final 24 h from each 5-day experiment. The light (dark) curve with open (solid) circles depicts the histogram from the control (high-CO_2) cases. See text for further details. For color version, see plate section.

relatively insensitive to the moist convection treatment (e.g., Fig. 7 and Table 2 of KT04).

Although it is not shown here, a similar intensity analysis based on maximum surface wind speeds also indicates higher-intensity storms under high-CO_2 conditions. In these experiments, the mean maximum surface wind intensity increased by 5.8% for high-CO_2 conditions. Based on the average change in SST of 1.75 °C between our control and high-CO_2 runs, our experiments indicated a normalized tropical cyclone wind intensity sensitivity of +3.3% per degree Celsius. Using central pressures from the model and inferring maximum sustained surface wind speeds following Landsea (1993), based on Kraft's (1961) analysis of Atlantic tropical cyclones, we obtained a slightly higher sensitivity of 3.7% per degree Celsius. These sensitivities are slightly less than the 5% per degree Celsius sensitivity reported by Emanuel (2005a) for his hurricane potential intensity theory, and are significantly less than the sensitivities inferred from recent observational studies, as will be discussed later. In

KT04, we also presented calculations of potential intensity changes for our environmental fields using both the Emanuel (1987, 1988) and the Holland (1997) methodologies. Those calculations indicated broadly similar sensitivity results from potential intensity theory, as compared to our model simulations (see KT04 for details).

7.3.3 Revised precipitation results

In KT04, three different types of precipitation measures for the simulated hurricanes were presented, each indicating enhanced rainfall rates for warmer, high-CO_2 conditions. The specific results reported in KT04 included statistics for an area-averaged near-storm rainfall rate (within 100 km of the storm center), the maximum precipitation rate anywhere in the model domain, and the average precipitation rate in a 5° latitude × 5° longitude inner mesh centered on the storm.

We have since discovered some problems with these precipitation statistics as reported in KT04. The first problem stems from the application of a spatial smoothing procedure once per simulation hour during the time integration of the hurricane model. The precipitation statistics were affected by the unrepresentative high values occurring once per hour, which were artifacts of the spatial smoothing procedure. The second problem was an incorrect description of the large-scale precipitation measure. Our large-scale rainfall measure from KT04 is now correctly identified (Table 7.1) as the average storm total precipitation averaged over the entire (70° × 70°) model domain, as opposed to just the 5° × 5° inner mesh.

Table 7.1 presents our revised precipitation statistics, which supersede the precipitation entries in Table 2 of KT04 (see the Appendix to this chapter for details). The problem related to spatial smoothing mentioned above had only a relatively minor effect on the percentage increase in storm-core rainfall induced by CO_2-related global warming, which was the main precipitation conclusion we emphasized in KT04. With the revised, more representative statistics discussed in the Appendix, we obtain an increase in storm-core rainfall of 21.6% for high-CO_2 conditions, compared with 18.3% for our original analysis in KT04. The percentage change is still fairly sensitive to the moist convection scheme used, varying from 18% to 27% for the three treatments analyzed (Table 7.1). The smoothing-induced problem significantly affected the absolute values of the precipitation rates as shown in Table 2 of KT04 and in some of the figures of that report. For example, the magnitudes of the precipitation rates shown in Figures 1, 8, and 14, and Table 1 (100 km radius) of KT04 overestimate the true time averages from the model by roughly 80%.

Table 7.1. *Revised precipitation statistics for KT04 simulations*[a]

	All convection schemes		HPAN		EMAN		KURI		Resolved	
	Control	Percent change	Control	Percent change	Control	Percent change	Control	Percent change	Control	Percent change
6-hour accumulated ($32{,}700\ km^2$ region; cm)	12.4	21.6%	12.8	26.5%	n/a	n/a	12.6	19.9%	11.8	18.0%
Maximum rate in domain	n/a	n/a	n/a	n/a	n/a	n/a	n/a	n/a	n/a	n/a
5-day accumulated (averaged over $70^\circ \times 70^\circ$ domain; cm)	1.62	6.7%	1.74	8.8%	1.27	8.7%	2.18	2.7%	1.28	8.6%

[a] HPAN, EMAN, and KURI refer to different moist convection physics schemes in the model, which were varied as a sensitivity test in KT04. "Resolved" refers to model runs with no convection parameterization for the model's inner grid so that only condensation processes resolved by the model are included. See KT04 for further details on the moist physics schemes.

The question arises whether the GFDL hurricane model has skill at predicting hurricane-related rainfall. Recently, Tuleya *et al.* (2007) and Marchok *et al.* (2007) have evaluated this aspect of the operational performance of the model using several rainfall measures. They found that the model has a high bias in terms of its inner-core (100 km radius) 6-hourly accumulated rainfall. The high bias they identified is over and above the (artificial) high bias we introduced in KT04, as discussed in Appendix 7.1. Despite the high bias identified by Marchok *et al.* (2007), they found the overall predictive skill of rainfall forecasts using the GFDL model to be competitive with that of other operational models. The operational models evaluated, including the Global Forecast System (GFS) and North American Mesoscale (NAM) models of the National Centers for Environmental Prediction and the GFDL hurricane model, each appear to have significant skill, relative to a "climatology/persistence" benchmark. The comparison benchmark consisted of a climatological hurricane rainfall rate pattern, decreasing radially outward from the storm center, which is projected along the storm's path. Their analysis also showed that the heavier rainfall totals (e.g., exceeding 9 inches' accumulation) were often not predicted at the correct locations by the models.

The heavy rainfall accumulations from the storms in the KT04 idealized experiments were generally confined to a swath within about 100 km of the storm track. This feature is well captured by our storm core precipitation measure described in Appendix 7.1. In the real world, areas of significant rainfall accumulation from hurricanes may not be as confined to the storm track region as they were in our idealized experiments. Under real-world conditions, interactions with extratropical weather systems, landfall effects, interactions with topography, stalling storm motion, and other phenomena (all of which are absent from our idealized experimental design), can lead to more spatially extensive regions with high rainfall accumulations. Future studies with less idealized design will likely produce examples of more areally extensive high-rainfall regions, in which case other aspects of the rainfall response can be examined in more detail.

A key physical mechanism that produces enhanced precipitation rates under warmer, high-CO_2 conditions in the GFDL hurricane model is enhanced boundary layer and lower tropospheric moisture associated with the warmer atmosphere. Since moisture convergence is an important component of the moisture budget for the model, the enhanced moisture leads to enhanced moisture convergence, and thus enhanced core precipitation rates, independent of the effect of intensified circulation. Storm intensification appears to be a secondary influence and acts to further enhance the moisture convergence.

To date, no observational evidence has been reported for an increase in precipitation from hurricane activity (e.g., Groisman *et al.*, 2004), although per-storm precipitation rates have not been evaluated. This is likely to be a challenging measurement and trend detection problem. Trenberth *et al.* (2005) reported a substantial increase during 1988–2003 in column-integrated atmospheric water vapor over the global oceans as derived from the special sensor microwave imager (SSM/I) satellite dataset. Thus it appears that tropical precipitable water vapor (an important ingredient of our simulated precipitation increase) is in fact increasing along with tropical SSTs in a manner consistent with the notion of approximately constant relative humidity, and in accord with model simulations of tropical relative humidity under CO_2 warming conditions (e.g., KT04).

7.3.4 Comparison of KT04 with observed intensity trends

In this section, we consider how our modeled hurricane intensity sensitivity compares with some recently reported observed trends in tropical cyclone (TC) measures.

Emanuel (2005a) introduced a power dissipation index (PDI) of tropical cyclones, based on the time-integrated cube of the maximum surface wind speeds (reported or inferred from central pressure reports and/or satellite data) for the Atlantic and Northwest Pacific tropical cyclone basins from the late 1940s to 2003. After adjusting for time-dependent biases due to changes in measurement and reporting practices, Emanuel reported an approximately 50% increase over the period of record in the annual mean maximum intensity (specifically, the velocity cubed) of the storms. This increase in intensity implies about a 15% increase in terms of wind speed ($1.15^3 = 1.52$). The PDI had a near doubling over the period, with contributions from increases in frequency, intensity, and mean storm duration. The low-pass filtered PDI series were significantly correlated with large-scale tropical SST indices for both basins.

A subsequent comment by Landsea (2005) resulted in adjustments, removing much of the large post-2000 upswing in the Atlantic PDI series through 2003. Emanuel (2005b) reported that these adjustments had a minimal impact on the Northwest Pacific results, or on the multi-basin series or on the correlations with SSTs. A revised and updated analysis (Emanuel, 2007) still shows a clear long-term rise in Atlantic PDI between ~1950 and 2005, correlated with increasing tropical Atlantic sea surface temperature.

Emanuel (2006) restricting the analysis to the Atlantic since about 1980, found a potential intensity increase of about 10% accompanying an SST

increase of about 0.5 °C, yielding a potential intensity sensitivity of about 20% per degree Celsius, using NCEP reanalyses of the large-scale climate conditions. Emanuel noted that the change in the actual intensities (average storm lifetime maximum wind speeds) was consistent with that of the potential intensity during this latter period in the Atlantic.

Mann and Emanuel (2006) presented a low-pass filtered time series of annual TC numbers for the Atlantic basin extending back into the late 1800s. This measure tracks the long-term variation in Atlantic MDR SSTs – an independently observed, but physically related, environmental variable – fairly closely, particularly for the century-scale warming trend. This correlation lends support to the notion that the trends in both series are real. On the other hand, one can question what impact changes in observing capabilities have had on the annual TC counts, particularly extending into the late 1800s. Landsea *et al.* (2004) had earlier estimated the number of "missed" Atlantic basin tropical storms and hurricanes per year to be on the order of zero to six for the period 1851–85 and zero to four for the period 1886–1910.

Webster *et al.* (2005) reported that the number of category 4 and 5 hurricanes has almost doubled globally over the past three decades. Although their analysis spans a shorter time period than Emanuel's, their results indicate that a substantial increase has occurred in all six tropical storm basins. In a follow-on study, Hoyos *et al.* (2006) found that the increasing trends in category 4 and 5 tropical cyclones are principally correlated with SST as opposed to other environmental factors. Chan (2006) extended the analysis of Webster *et al.* for the Northwest Pacific basin back to earlier years and argued that the "trend" in that basin is part of a large interdecadal variation. Chan used unadjusted data from the earlier part of the record, in contrast to the adjustments for this period proposed by Emanuel (2005a) for this basin.

A precise comparison of the TC statistics in the above studies with those in the KT04 study is beyond the scope of the present work. The experimental design in KT04 does not consider frequency changes, for example, and so is not directly comparable to the Mann and Emanuel (2006) finding. The PDI measures reported in Emanuel's studies depend on frequency and duration as well as on the intensities of storms. The findings of Webster *et al.* show a redistribution of hurricane intensities preferentially toward more frequent occurrences of category 4 and 5 storms, but no discernible trend in maximum intensities was found. Therefore, for comparison to KT04, we focus on the observed intensity or potential intensity changes as reported in Emanuel (2005a) and Emanuel (2006).

Based on Emanuel (2005a), we assume that a 15% increase in maximum surface wind speeds, as inferred from that study, is representative of the multi-basin change of intensity over the second half of the twentieth century and

corresponds to a tropical (30° S–30° N) SST increase of approximately 0.5 °C. This figure yields an approximate sensitivity of 30% per degree Celsius. Alternatively Emanuel's (2006) Atlantic observed potential intensity trend since about 1980 corresponds to a sensitivity of about 20% per degree Celsius. In comparison, the mean intensity result from KT04 is a 5.8% increase in maximum surface wind speeds for a CO_2-induced warming of 1.75 °C, yielding a sensitivity of 3.3% per degree Celsius (or 3.7% if winds are inferred from surface pressure). Emanuel (2005a) reported a theoretically derived potential intensity sensitivity of 5% per degree Celsius, similar to our model results. Although these are admittedly crude comparisons, large differences in sensitivity (by a factor of roughly 5–8 in these examples) remain to be reconciled between our model results and Emanuel's observational findings. Emanuel (2005a, 2006) presented a similar discussion on this topic, proposing that surface wind speed changes could help reconcile the observed Atlantic intensity data with existing theory.

We speculate that the large difference between our model and Emanuel's observed trends in the apparent sensitivity of TC intensity to SST changes may arise from three potential causes: (1) an overestimation of the observed trend due to potential data problems, (2) an underestimation by our model of the sensitivity of hurricane intensities to CO_2-induced SST changes, or (3) impacts of changes in other related environmental factors besides SST on hurricane intensity trends. Each of these possibilities is elaborated on below.

As a first possibility, we speculate that the reported observed intensity trends are overestimated owing to data problems. A recurrent problem in climate studies examining past records for evidence of trends is the impact of changes in instrumentation and reporting practices, which can produce artificial trends. Emanuel (2005a) provided considerable discussion of this issue in the supplemental notes to his study, including a description of adjustments that he made to the data to obtain a more homogeneous record. Webster *et al.* (2005) and Hoyos *et al.* (2006) restricted their analysis to the satellite era in an effort to reduce data homogeneity problems. However, the possibility that other data-related problems are significantly biasing the reported trends continues to be a major issue of concern in the tropical cyclone historical database community (e.g., Landsea *et al.*, 2004; Landsea, 2005; Knaff and Sampson, 2006; Landsea *et al.*, 2006; Kossin *et al.*, 2007). These concerns have focused particularly on basins outside of the Atlantic and on Atlantic intensities prior to the satellite era. Thus Emanuel's (2006) intensity results for the Atlantic basin for the period since about 1980 are likely more reliable than multi-basin measures of intensity changes.

Model deficiencies are a second possible explanation of the differences between observed trends and the modeling studies. Could these lead to an

unrealistically low sensitivity to SST changes? In KT04, we presented alternative calculations of CO_2 warming-induced intensity changes based on the potential intensity theories of Emanuel (1987, 2000) and Holland (1997). Despite differences between these theories in the sensitivity of potential intensity to different environmental factors (e.g., Camp and Montgomery, 2001), both formulations gave results that were similar to those of our model calculations, again supporting the general magnitude of our model estimates. The performance of these hurricane intensity frameworks has been assessed to varying degrees based on geographical or seasonal variations in real-world tropical cyclone intensities (e.g., Emanuel, 1987; Holland, 1997; Knutson *et al.*, 1998; Emanuel, 2000; Tonkin *et al.*, 2000). The skill of the GFDL hurricane model for operational intensity forecasts and its relevance for the research issue assessed here has been a subject of debate (Knutson and Tuleya, 2005; Michaels *et al.*, 2005). The 9 km horizontal grid spacing of our model could conceivably be an important limitation of our sensitivity results: a topic that deserves further study. However, we see little evidence at this time that the model used in KT04 is under-sensitive to environmental changes to a degree large enough to explain the factor of 5–8 discrepancy with Emanuel's (2005a, 2006) reported intensity trends.

A third possible explanation of the differences between the results of these studies is that our previous discussion, by focusing on SST sensitivity alone, is too simplistic. In particular, other factors besides SST (e.g., environmental lapse rate,[2] convective available potential energy [CAPE[3]], or tropical cyclone potential intensity) may have changed over the past 25–50 years in a manner different from that simulated by climate models in response to CO_2-only forcing. For example, models and theory indicate that an enhanced warming of the troposphere relative to the sea surface under climate change should act to limit any increase of hurricane intensity for a given SST increase. Therefore, if the tropical upper troposphere, on the whole or in part, has not warmed more than near the surface for some reason during recent decades, the estimated TC intensity change obtained by scaling the KT04 results to recent observed tropical SST changes would be too small. Aside from potential intensity, other investigators emphasize the role of vertical wind shear or other dynamical influences on TC activity (e.g., Gray, 1990; Goldenberg *et al.*, 2001; Bell and Chelliah, 2006). These latter studies suggest that a variety of thermodynamic and dynamic influences, in addition to SST and potential intensity, could be

[2] Lapse rate is the rate of change of temperature with height in the atmosphere.
[3] Convective available potential energy is the maximum energy available to an ascending idealized parcel according to parcel theory, and is an integrated measure of moist atmospheric stability in the vertical direction.

influencing any observed trends in TC activity. Holland and Webster (2007) interpret the strong increase in Atlantic hurricane activity in recent years as arising from a combination of a long-term upward trend in total numbers of Atlantic TCs forced by greenhouse warming and an internal oscillation currently favoring more low-latitude developments, which results in a greater proportion of TCs becoming major hurricanes. From these perspectives, explaining past variations of tropical cyclone indices would require more sophisticated statistical or modeling approaches than KT04 to account for the relative roles of these various factors.

We now briefly return to the question of whether an increasingly unstable tropical atmosphere, as is implied by trend profiles computed by using radiosonde data (e.g., Santer *et al.*, 2005) could help explain the large increase in tropical cyclone intensities. Unfortunately, the picture emerging to date from observational studies of trends in tropical tropospheric lapse rates, CAPE, and potential intensity is inconclusive. For example, Gettelman *et al.* (2002) found a preponderance of upward trends in tropical CAPE since roughly the early 1960s. DeMott and Randall (2004) examined a larger number of tropical stations over a shorter period (1973–99) and reported a more evenly divided mixture of increasing and decreasing CAPE trends. Trenberth (2005) questioned the reliability of the radiosonde data in DeMott and Randall's larger sample. Free *et al.* (2004), using a selected set of 14 tropical island radiosonde stations, found only small, statistically insignificant trends in potential intensity over the periods 1975–95 and 1980–95. Emanuel's (2006) reported 10% increase in Atlantic Main Development Region potential intensity since about 1980 was based on HadISST and NCEP reanalysis data. The relation of this multidecadal increase in potential intensity to century-scale tropical SST warming (e.g., Mann and Emanuel, 2006) remains unclear. Also, Santer *et al.* (2005) suggest that there are further problems with radiosonde-derived and satellite-derived temperature trends for the period since 1979 – a conclusion also receiving some support from two additional recent studies, which examined issues with radiosonde-based observations (Sherwood *et al.*, 2005) and satellite-based analyses (Mears and Wentz, 2005). Such problems could conceivably affect trends in atmospheric stability or potential intensity derived from various reanalysis products.

In summary, we have examined three general possibilities for reconciling our model results for intensity with recently reported observational work, but we are unable to reconcile those differences at this time. Both our model and our experimental design may be questioned. On the other hand, they may also have contributed to the discrepancies, particularly for data from outside of the Atlantic basin, or from the presatellite era (pre-1966).

7.4 Conclusions

The main conclusions of this chapter are as follows.

- The tropical Atlantic MDR has warmed by several tenths of a degree Celsius over the twentieth century, including a more rapid rise than for global temperature since about 1970. Coupled model historical simulations using current best estimates of radiative forcings suggest that the warming trend in the MDR may contain a significant contribution from anthropogenic forcing, including increases in atmospheric greenhouse gas concentrations.
- The GFDL hurricane model, in an idealized setting, simulates that a CO_2-induced warming of 1.75 °C causes hurricanes to have increased intensities by 5.8% in terms of surface wind speeds, 14% in terms of central pressure fall, or about one half category on the Saffir–Simpson scale. The 1.75 °C warming found in KT04 is the three-basin average warming simulated by nine global climate models in response to a 1% per year compounded buildup of CO_2 over 80 years: a strong though not extreme scenario for future global mean radiative forcing. Normalizing by the SST change and using wind speeds inferred from central pressure, the wind speed sensitivity of the model is 3.7% per degree Celsius. The storm intensification due to increased SSTs exceeds the moderating effects of more stable tropospheric lapse rates in these hurricane model experiments.
- A measure of the primary core of accumulated precipitation from the idealized hurricanes (the accumulated precipitation during the final 6 hours over a 32,700 km^2 region) shows a 21.6% increase under high-CO_2 conditions.
- Our simulated storm intensities are substantially less sensitive to SST changes compared with historical trends of TC intensity or potential intensity as reported by Emanuel (2005a, 2006). We speculate that the large (factor of 5–8) difference in apparent sensitivity may arise from three potential causes: (i) an overestimation of the observed trends due to potential data problems, (ii) an underestimation by our model of the sensitivity of hurricane intensities to CO_2 warming-induced SST changes, or (iii) impacts of changes in other environmental factors besides SST on hurricane intensity or potential intensity trends. We are unable to reconcile these differences at this stage.

Future work on this topic should include both more extensive evaluations of historical tropical cyclone databases, and simulation efforts aimed at increasing the realism of tropical cyclone climatological behavior. For example, we have not addressed issues of tropical cyclogenesis (frequency), duration, or tracks under modified climate conditions. In the KT04 study, the effects on intensity of wind shear, landfall, topography, and interactions with other weather systems were not addressed.

As a final reminder of the complexities that can arise in the case of Atlantic basin hurricanes, recent climate model simulations point to a significant role for anthropogenic forcing in producing both past and future drought conditions in

the Sahel (Held *et al.*, 2005). West African monsoonal activity is believed to be related to Atlantic hurricane activity (e.g., Gray, 1990; Bell and Chelliah, 2006), and indices of atmospheric dust cover emanating from the Sahara region also correlate significantly with the number of TC days (Evans *et al.*, 2006). Furthermore, our results suggest that the low-frequency variability in the MDR, apart from the trend, may contain substantial contributions from both radiative forcing (natural and anthropogenic) and internally generated climate variability. Efforts are now ongoing to attempt to understand and evaluate this complex set of physical mechanisms, which should lead to increased understanding of these important aspects of the tropical climate.

References

Bell, G. D., and Chelliah, M. (2006). Leading tropical modes associated with interannual and multidecadal fluctuations in North Atlantic hurricane activity. *Journal of Climate*, **19**, 590–612.

Broccoli, A. J., Dixon, K. W., Delworth, T. L., Knutson, T. R., and Stouffer, R. J. (2003). Twentieth-century temperature and precipitation trends in ensemble climate simulations including natural and anthropogenic forcing. *Journal of Geophysical Research*, **108**, D24, 4798, doi:10.1029/2003JD003812.

Brohan, P., Kennedy, J. J., Haris, I., Tett, S. F. B., and Jones, P. D. (2006). Uncertainty estimates in regional and global observed temperature changes: a new dataset from 1850. *Journal of Geophysical Research*, **111**, D12106, doi:10.1029/2005JD006548.

Camp, J. P., and Montgomery, M. T. (2001). Hurricane maximum intensity: past and present. *Monthly Weather Review*, **129**, 1704–17.

Chan, J. C. L. (2006). Comment on "Changes in tropical cyclone number, duration, and intensity in a warming environment". *Science*, **311**, 1713.

DeMott, C. A., and Randall, D. A. (2004). Observed variations of tropical convective available potential energy. *Journal of Geophysical Research*, **109**, D02102, doi:10.1029/2003JD003784.

Emanuel, K. A. (1987). The dependence of hurricane intensity on climate. *Nature*, **326**, 483–5.

Emanuel, K. A. (1988). The maximum intensity of hurricanes. *Journal of Atmospheric Science*, **45**, 1143–55.

Emanuel, K. (2000). A statistical analysis of tropical cyclone intensity. *Monthly Weather Review*, **128**, 1139–52.

Emanuel, K. A. (2005a). Increasing destructiveness of tropical cyclones over the past 30 years. *Nature*, **436**, 686–8.

Emanuel, K. A. (2005b). Emanuel replies. *Nature*, **438**, doi:10.1038/nature04427.

Emanuel, K. (2006). Environmental influences on tropical cyclone variability and trends. *Proceedings of 27th AMS Conference on Hurricanes and Tropical Meteorology*, No. 4.2. Available online at http://ams.confex.com/ams/pdfpapers/107575.pdf.

Emanuel, K. (2007). Environmental factors affecting tropical cyclone power dissipation. *Journal of Climate* (in press).

Evans, A., Dunion, J., Foley, J. A., Heidinger, A. K., and Velden, C. S. (2006). New evidence for a relationship between Atlantic tropical cyclone activity and African

dust outbreaks. *Geophysical Research Letters*, **33**, L19813, doi:10.1029/2006GL026408.

Free, M., Bister, M., and Emanuel, K. (2004). Potential intensity of tropical cyclones: comparison of results from radiosonde and reanalysis data. *Journal of Climate*, **17**, 1722–7.

Gettelman, A., Seidel, D. J., Wheeler, M. C., and Ross, R. J. (2002). Multidecadal trends in tropical convective available potential energy. *Journal of Geophysical Research*, **107**, 4606, doi:10.1029/2001JD001082.

Goldenberg, S. B., Landsea, C. W., Mestas-Nuñez, A.M., and Gray, W. M. (2001). The recent increase in Atlantic hurricane activity: causes and implications. *Science*, **293**, 474–9.

Gray, W. M. (1990). Strong association between West African rainfall and U.S. landfall of intense hurricanes. *Science*, **249**, 1251–6.

Groisman, P. Y., Knight, R. W., Karl, T. R., *et al.* (2004). Contemporary changes of the hydrological cycle over the contiguous United States: trends derived from *in situ* observations. *Journal of Hydrometeorology*, **5**, 64–85.

Held, I. M., Delworth, T. L., Lu, J., Findell, K. L., and Knutson, T. R. (2005). Simulation of Sahel drought in the twentieth and twenty-first centuries. *Proceedings of the National Academy of Sciences, USA*, **102**(50), 17 891–6.

Holland, G. J. (1997). The maximum potential intensity of tropical cyclones. *Journal of Atmospheric Science*, **54**, 2519–41.

Holland, G. J., and Webster, P. J. (2007). Heightened tropical cyclone activity in the North Atlantic: natural variability or climate trend? *Philosophical Transactions of the Royal Society A*, doi:10.1098/rsta.2007.2083.

Hoyos, C. D., Agudelo, P. A., Webster, P. J., and Curry, J. A. (2006). Deconvolution of the factors contributing to the increase in global hurricane intensity. *Science*, **312**, 94–7.

International Ad Hoc Detection and Attribution Group (IADAG) (2005). Detecting and attributing external influences on the climate system: a review of recent advances. *Journal of Climate*, **18**, 1291–314.

Jones, P. D., and Moberg, A. (2003). Hemispheric and large-scale surface air temperature variations: an extensive revision and an update to 2001. *Journal of Climate*, **16**, 206–23.

Knaff, J. A., and Sampson, C. R. (2006). Reanalysis of West Pacific tropical cyclone maximum intensity 1966–1987. *Proceedings of 27th AMS Conference on Hurricanes and Tropical Meteorology*, No. 5B.5. Available online at http://ams.confex.com/ams/pdfpapers/108298.pdf.

Knutson, T. R., and Tuleya, R. E. (2004) (KT04). Impact of CO_2-induced warming on simulated hurricane intensity and precipitation: sensitivity to the choice of climate model and convective parameterization. *Journal of Climate*, **17**, 3477–95.

Knutson, T. R., and Tuleya, R. E. (2005). Reply. *Journal of Climate*, **18**(23), 5183–7.

Knutson, T. R., Delworth, T. L., Dixon, K. W., *et al.* (2006) (K06). Assessment of twentieth-century regional surface temperature trends using the GFDL CM2 coupled models. *Journal of Climate*, **19**(9), 1624–51.

Knutson, T. R., Tuleya, R. E., and Kurihara, Y. (1998). Simulated increase of hurricane intensities in a CO_2-warmed climate. *Science*, **279**, 1018–21.

Knutson, T. R., Tuleya, R. E., Shen, W., and Ginis, I. (2001). Impact of CO_2-induced warming on hurricane intensities as simulated in a hurricane model with ocean coupling. *Journal of Climate*, **14**, 2458–68.

Kossin, J. P., Knapp, K. R., Vimont, D. J., Murnane, R. J., and Harper, B. A. (2007). A globally consistent reanalysis of hurricane variability and trends, *Geophysical Research Letters*, **34**, LO4815, doi:10.1029/2006GL028836.

Kraft, R. H. (1961). The hurricane's central pressure and highest wind. *Marine Weather Log*, **5**, 155.
Landsea, C. W. (1993). A climatology of intense (or major) Atlantic hurricanes. *Monthly Weather Review*, **121**, 1703–13.
Landsea, C. W. (2005). Hurricanes and global warming. *Nature*, **438**, doi:10.1038/nature04477.
Landsea, C. W. (2007). Counting Atlantic tropical cyclones back to 1900. *EOS*, **88**, 197, 202.
Landsea, C. W., Anderson, C., Charles, N., *et al.* (2004). The Atlantic hurricane database re-analysis project: documentation for the 1851–1910 alterations and additions to the HURDAT database. In *Hurricanes and Typhoons: Past, Present, and Future*, ed. R. J. Murnane and K.-B. Liu. New York: Columbia University Press, pp. 177–221.
Landsea, C. W., Harper, B. A., Hoarau, K., and Knaff, J. A. (2006). Can we detect trends in extreme tropical cyclones? *Science*, **313**, 452–4.
Mann, M., and Emanuel, K. (2006). Atlantic hurricane trends linked to climate change. *Eos*, **87**, 233–41.
Marchok, T., Rogers, R., and Tuleya, R. (2007), Validation schemes for tropical cyclone quantitative precipitation forecasts: evaluation of operational models for US landfalling cases. *Weather and Forecasting*, **22**, 726–46.
Mears, C. A., and Wentz, F. J. (2005). The effect of diurnal correction on satellite-derived lower tropospheric temperature. *Science*, **309**, 1548–51.
Meehl, G. M., Washington, W. M., Amman, C. M., *et al.* (2004). Combinations of natural and anthropogenic forcings in twentieth-century climate. *Journal of Climate*, **17**, 3721–7.
Michaels, P. J., Knappenberger, P. C., and Landsea, C. (2005). Comments on "Impacts of CO_2-induced warming on simulated hurricane intensity and precipitation: sensitivity to the choice of climate model and convective scheme." *Journal of Climate*, **18**, 5179–82.
Parker, D. E., Folland, C. K., and Jackson, M. (1995). Marine surface temperature: observed variations and data requirements. *Climate Change*, **31**, 559–600.
Rayner, N. A., Parker, D. E., Horton, E. B., *et al.* (2003). Global analyses of sea surface temperature, sea ice, and night marine air temperature since the late nineteenth century. *Journal of Geophysical Research*, **108** (D14), 4407, doi:10.1029/2002JD002670.
Santer, B. D., *et al.* (2005). Amplification of surface temperature trends and variability in the tropical atmosphere. *Science*, **309**, 1551–6.
Santer, B. D., *et al.* (2006). Forced and unforced ocean temperature changes in Atlantic and Pacific tropical cyclogenesis regions. *Proceedings of the National Academy of Sciences, USA*, **103**, 13905–10, 10.1073/pnas.0602861103.
Shen, W., Tuleya, R. E., and Ginis, I. (2000). A sensitivity study of the thermodynamic environment on GFDL model hurricane intensity: implications for global warming. *Journal of Climate*, **13**, 109–21.
Sherwood, S. C., Lanzante, J. R., and Meyer, C. L. (2005). Radiosonde daytime biases and late-twentieth-century warming. *Science*, **309**, 1556–9.
Smith, T. M., and Reynolds, R. W. (2003). Extended reconstruction of global sea surface temperatures based on COADS data (1854–1997). *Journal of Climate*, **16**, 1495–510.
Smith, T. M., and Reynolds, R. W. (2004). Improved extended reconstruction of SST (1854–1997). *Journal of Climate*, **17**, 2466–77.
Tonkin, H., Holland, G. J., Holbrook, N., and Henderson-Sellers, A. (2000). An evaluation of thermodynamic estimates of climatological maximum potential tropical cyclone intensity. *Monthly Weather Review*, **128**, 746–62.

Trenberth, K. (2005). Uncertainty in hurricanes and global warming. *Science*, **308**, 1753–4.
Trenberth, K. E., and Shea, D. J. (2006). Atlantic hurricanes and natural variability in 2005. *Geophysical Research Letters*, **33**, L12704, doi:10.1029/2006GL026894.
Trenberth, K. E., Fasullo, J., and Smith, L. (2005). Trends and variability in column-integrated atmospheric water vapor. *Climate Dynamics*, **24**, 741–58.
Tuleya, R. E., DeMaria, M., and Kuligowski, R. (2007). Evaluation of GFDL and simple statistical model rainfall forecasts for U.S. landfalling tropical storms. *Weather and Forecasting*, **22**, 56–70.
Vecchi, G. A., and Soden, B. J. (2007). Increased tropical Atlantic wind shear in model projections of global warming. *Geophysical Research Letters*, **34**, L08702, doi:10.1029/2006GL028905.
Webster, P. J., Holland, G. J., Curry, J. A., and Chang, H. -R. (2005). Changes in tropical cyclone number, duration, and intensity in a warming environment. *Science*, **309**, 1844–6.
Zhang, R., and Delworth, T. L. (2005). Simulated tropical response to a substantial weakening of the Atlantic thermohaline circulation. *Journal of Climate*, **18**(12), 1853–60.

APPENDIX 7.1 REVISED PRECIPITATION STATISTICS

Inspection of high-frequency (every model time step) precipitation time series from the hurricane model simulations of KT04 reveals periodic "spikes" in precipitation rates. The spikes occur just after application, once per integration hour, of a 1–2–1 spatial filter to the mass and pressure fields of the model during its time integration. Use of time-accumulated or time-averaged (across all time steps) precipitation fields largely eliminates the effect of this artifact of the numerical smoothing.

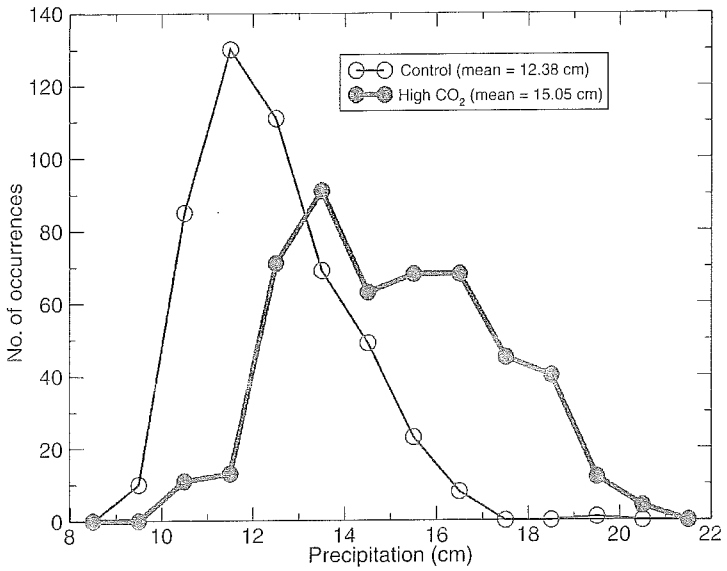

Figure 7.5. As Figure 7.4, but for precipitation (centimeters) averaged over the 102 model grid points (comprising a 32,700 km^2 area) with highest accumulated precipitation during the final 6 h of the 5-day hurricane model integrations.

However, the 100 km radially averaged precipitation rate statistic in KT04 was based on instantaneous precipitation fields from the model, and these coincidentally were computed at a time step of the model integration in which a spike in precipitation rate was occurring (i.e., at exactly hour 120). Thus the 100 km rate measure in KT04 turns out to be unrepresentative of the true average precipitation rates in the model. (Note that such spikes are not evident in storm intensity metrics for the model.)

To assess the impact of this problem on our earlier results, we reanalyzed the precipitation data and created an alternative storm-core precipitation measure from a different (time-accumulated) archived field: the 6-hour accumulated rainfall. This field was archived for each of the four cumulus convection treatments except for the Emanuel scheme. Therefore, our revised analysis and comparisons are limited to three of the four convection treatments used in KT04 (i.e, the PAN, KURI, and resolved convection schemes, see Table 7.1.)

Maps of 6-hour accumulated rainfall from the experiments (not shown) are dominated by an oblong-shaped maximum along the 6-hour storm track. Because of the oblong shape of this feature, we chose not to compute a simple circular average as in KT04 (where we were using instantaneous fields). Instead, we sorted the 6-hour accumulated precipitation field grid points (for the final 6-hour period) from largest to smallest and then averaged over the highest 102 values (out of a total of 202,500 grid points), comprising an area of 32,700 km^2, or slightly more than the area covered by a circular region of radius 100 km.

Comparisons between the revised and original measures indicate that the original control run precipitation measure (converted to units of centimeters per 6 hours for comparison) is artificially inflated by roughly 80%, which we interpret as primarily due to sampling the peaks or spurious spikes in the time series associated with the spatial smoothing procedure. However, we find that the percentage changes from control to high-CO_2 samples are quite similar for the new and original precipitation measures. The revised analysis (summarized in Figure 7.5 and Table 7.1) yields a 21.6% aggregate increase (high CO_2 vs. control) for the three available convection schemes, as compared with 17.1% for those same three schemes using the original 100 km radius instantaneous measure, and 18.3% for the original measure averaged over all four moist convection treatments.

The "maximum precipitation rate in the domain" measure was a secondary precipitation statistic presented in KT04 aimed at exploring the small-scale local maxima in precipitation. This statistic was also affected by the precipitation spikes. In this case, we could not reconstruct a suitable alternative from the available archived data. Therefore, we recommend that the maximum precipitation rate in domain statistics in KT04 not be considered quantitatively reliable.

The "inner nest average" precipitation measure in KT04 was not described accurately in the text or in Table 2 of KT04. In fact, this statistic should have been labeled as the "5-day total accumulated rainfall (in centimeters) area-averaged over the entire model domain ($70^\circ \times 70^\circ$)." Again, this statistic was a secondary precipitation measure designed to contrast how the larger-scale precipitation rates changed in response to CO_2-induced warming in comparison to the storm-core rainfall. The reported control run values in Table 2 of KT04 (e.g., 1.62 for "all convection schemes") are correct as given, but the units are centimeters, and the description should have been as corrected above. This statistic, being an accumulated precipitation over the storm lifetime, is only minimally affected by the spatial smoothing issue discussed above.

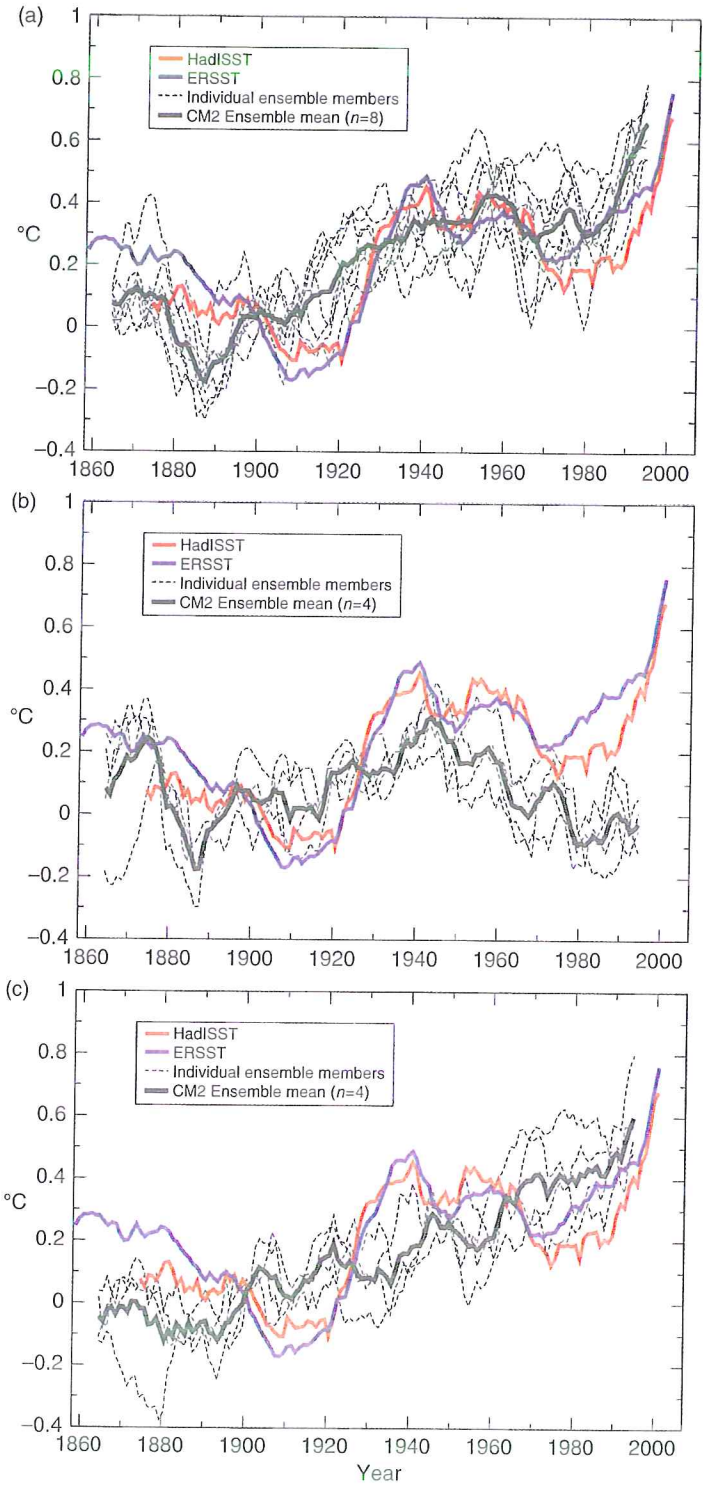

Figure 7.2. Observed sea surface temperature variations in the MDR from HadISST (red) and ERSST (blue) datasets vs. CM2 historical climate simulations using (a) all forcings, (b) natural forcings only, or (c) anthropogenic forcings only. Ten-year running mean anomalies for the August–October season, referenced to 1881–1920 means in degrees Celsius, are shown. Black dashed curves are individual CM2.0 or CM2.1 ensemble members; thick black curves are the CM2.0/CM2.1 ensemble means ($n = 8$ experiments with all forcings; $n = 4$ experiments with natural- or anthropogenic-only forcings).

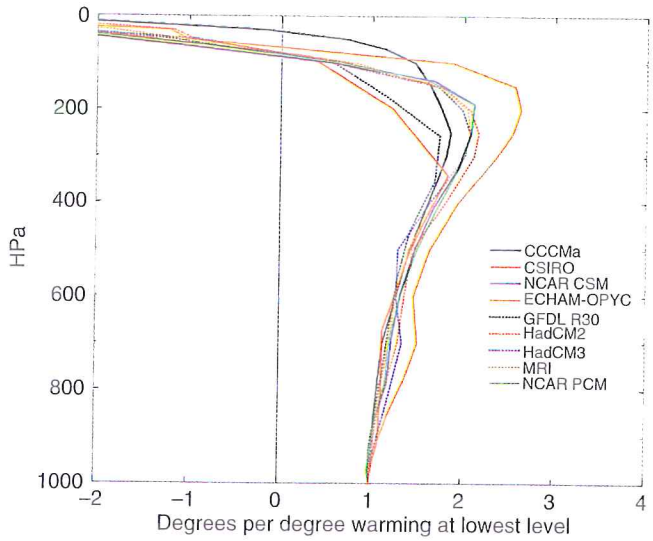

Figure 7.3. Vertical profiles of normalized atmospheric temperature change (high-CO_2 minus control) zonally averaged over 20° N–20° S from a set of transient +1% per year CO_2 increase experiments using nine global climate models. The difference is based on years 61–80 of the high-CO_2 runs minus years 61–80 of the control runs for each model (see legend). The difference at each model level is normalized by dividing by the difference at the lowest available level for that model.

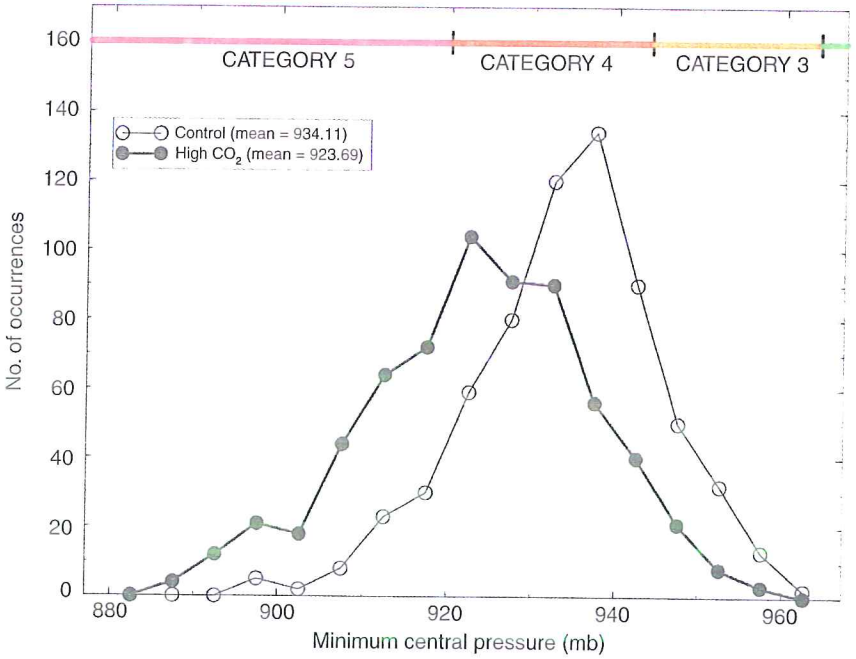

Figure 7.4. Frequency histogram showing hurricane intensity results (millibars) aggregated across all 1,296 experiments of KT04 (9 GCMs, 3 basins, 4 parameterizations, 6-member ensembles). The histograms are formed from the minimum central pressures, averaged over the final 24 h from each 5-day experiment. The light (dark) curve with open (solid) circles depicts the histogram from the control (high-CO_2) cases. See text for further details.